17th Brazilian Congress of Thermal Sciences and Engineering
November 25th-28th, 2018, Águas de Lindóia, SP, Brazil

ENCIT-2018-XXXX
ANALYSIS OF THERMOCLINE STORAGE TANK CONFIGURATIONS FOR CONCENTRATED SOLAR POWER PLANTS

Fernando Andrade Rodrigues
Marcelo J. S. de Lemos
Departamento de Energia, Instituto Tecnológico de Aeronáutica – ITA, 12228-900 São José dos Campos, SP, Brasil
ferar@ita.br
delemos@ita.br

Abstract. *The goal of this work is to investigate the thermal behavior of different configurations of a thermal energy storage system for a concentrated solar power plant filled with solid porous material. In order to accomplish this goal, a time sensitive model that describes turbulent flow in a hybrid medium(porous/clear) with both forced and natural convection will be used. Different tank aspect ratios and boundary conditions are expected to be analyzed. The model will be validated using published experimental data.*

Keywords: *Heat Transfer, Concentrated Solar Power, Thermal Energy Storage, Thermocline*

1. INTRODUCTION

Energy consumption on the interconnected Brazilian national grid is expected to grow 42% in the next 10 years, according to the Empresa de Pesquisa Energética (EPE, 2015) report from 2015. Following national and international tendencies it can be anticipated that some of this demand will be supplied by new renewable energy generation plants. Efficient renewable energy production systems must be developed to accomplish this goal and solar energy is amongst the most promising technology solutions to reduce environmental impact and fossil fuel consumption.

Solar energy generation is divided in two groups, solar photovoltaic (PV) and concentrated solar power (CSP). Solar PV directly converts solar energy into electricity using solar cells (Py, Azoumah, & Olives, 2013). CSP systems use solar towers, parabolic troughs or Fresnel reflectors to concentrate solar energy and heat up a work fluid to high temperatures and then send it to a regular steam power plant (International Energy Agency, 2016). CSP systems can be integrated with a thermal energy storage (TES) system and proceed to generate power during nighttime, which is an advantage over solar PV systems that still provide a technological challenge for efficient energy storage (Xu, Li, & Chan, 2015).

TES in CSP plants is paramount for the feasibility of this technology since it can shift energy production to peak demand times and through periods with intermittent cloud cover. Therefore, with the addition of a TES system CSP plants can continue to produce power even through periods without direct solar radiation (Pilkington Solar International GmbH, 2000).

This project focuses on the development and application of a model that simulate the thermal behavior of a reservoir for thermal energy storage filled with solid permeable material. The model will consider a turbulent flow in a hybrid medium (clear/porous), forced convection in a ventilated cavity with fluid inlet and outlet and natural convection due to buoyancy. The two-energy equation model will be used to evaluate heat transfer between the solid and fluid phases. Dynamic behavior of the system will be evaluated through the transient temperature variation. Turbulent flow and heat transfer in porous media will be modelled using the macroscopic two-energy equation model (M. B. Saito & de Lemos, 2010).

Previous work using these models was already published by the research group (LCFT/ITA) on turbulent flow in porous media (Pedras & de Lemos, 2001a) and hybrid media (Santos & de Lemos, 2006), with heat transfer due to forced convection (Rocamora & de Lemos, 2000) and natural convection (Braga & De Lemos, 2004), with extensive documentation in (Marcelo J. S. de Lemos, 2012). The present work will unite those models and add temporal variation while adding the specific application for TES systems.

2. NUMERICAL MODEL

2.1 Transport Equations

For an incompressible fluid the governing flow and energy equations are given by:

Continuity equation:

$$\nabla \cdot \mathbf{u} = 0 \tag{1}$$

Momentum Equation:

$$\rho\left[\frac{\partial \mathbf{u}}{\partial t} + \nabla \cdot (\mathbf{u}\mathbf{u})\right] = -\nabla p + \mu \nabla^2 \mathbf{u} \tag{2}$$

Energy equation – Fluid Phase

$$(\rho c_p)_f \left[\frac{\partial T_f}{\partial t} + \nabla \cdot (\mathbf{u} T_f)\right] = \nabla.(k_f \nabla T_f) + S_f \tag{3}$$

Energy Equation – Solid Phase

$$(\rho c_p)_s \frac{\partial T_s}{\partial t} = \nabla.(k_s \nabla T_s) + S_s \tag{4}$$

where the subscripts s and f refer to the solid and fluid phase, respectively, T is the temperature, k is the thermal conductivity c_p is the specific heat and S is the heat generation term.

2.2 Double decomposition of variables

In the work developed in (Pedras & de Lemos, 2000, 2001b, 2003) the idea of double decomposition was introduced and described so that macroscopic transport equations which described turbulent flow in porous media could be obtained. The concept consists of a simultaneous application of time and volume averaged operators for a given property φ , the operators are:

$$\overline{\varphi} = \frac{1}{\Delta t}\int_t^{t+\Delta t} \varphi dt \ , \ \text{with} \quad \varphi = \overline{\varphi} + \varphi' \tag{5}$$

$$\langle \varphi \rangle^i = \frac{1}{\Delta V_f}\int_{\Delta V_f} \varphi dV \ ; \quad \langle \varphi \rangle^v = \phi \langle \varphi \rangle^i \ ;$$

$$\phi = \frac{\Delta V_f}{\Delta V}, \quad \text{with} \quad \varphi = \langle \varphi \rangle^i + {}^i\varphi \tag{6}$$

where ΔV_f is the fluid volume contained in a representative elementary volume (REV) ΔV , $\langle \varphi \rangle^i$ is the intrinsic average and $\langle \varphi \rangle^v$ is the volume average.

Double decomposition consists of merging equations (5) and (6), by means of the following:

$$\overline{\langle \varphi \rangle^i} = \langle \overline{\varphi} \rangle^i \ ; \quad {}^i\overline{\varphi} = \overline{{}^i\varphi} \ ; \quad \langle \varphi' \rangle^i = \langle \varphi \rangle^{i'} \tag{1}$$

$$\left.\begin{aligned} \varphi' &= \langle \varphi' \rangle^i + {}^i\varphi' \\ {}^i\varphi &= \overline{{}^i\varphi} + {}^i\varphi' \end{aligned}\right\} \ \text{where} \ {}^i\varphi' = \varphi' - \langle \varphi' \rangle^{i'} = {}^i\varphi - \overline{{}^i\varphi} \tag{2}$$

Thus, the given property φ can be represented by either (9) or (10):

$$\varphi = \overline{\langle\varphi\rangle^{i}} + \langle\varphi\rangle^{i'} + \overline{{}^{i}\varphi} + {}^{i}\varphi' \tag{3}$$

$$\varphi = \langle\overline{\varphi}\rangle^{i} + {}^{i}\overline{\varphi} + \langle\varphi'\rangle^{i} + {}^{i}\varphi' \tag{4}$$

where the term ${}^{i}\varphi'$ can be interpreted both as the time fluctuation of the spatial deviation and as the spatial deviation of the time fluctuation of the given property φ.

2.3 Macroscopic flow equations

Using the double decomposition concept, the operators in (5) and (6) can be applied, simultaneously, in the governing equations (1) and (2) which yields macroscopic equations for turbulent flow. Subsequently, a volume integration over a REV is performed to obtain:

Continuity equation:

$$\nabla \cdot \overline{\mathbf{u}}_D = 0 \tag{11}$$

where $\overline{\mathbf{u}}_D$ is the average surface velocity, also known as Darcy's velocity. The Dupuit-Forchheimer relationship, $\mathbf{u}_D = \phi\langle\mathbf{u}\rangle^{i}$, is used in equation (11), where ϕ is the porosity of the porous medium and $\langle\mathbf{u}\rangle^{i}$ represents the intrinsic average of the local velocity vector **u.**(Gray & Lee, 1977)

Momentum Equation:

$$\rho\left[\frac{\partial\overline{\mathbf{u}}_D}{\partial t} + \nabla\cdot\left(\frac{\overline{\mathbf{u}}_D\overline{\mathbf{u}}_D}{\phi}\right)\right] = -\nabla(\phi\langle\overline{p}\rangle^{i}) + \mu\nabla^2\overline{\mathbf{u}}_D + \nabla\cdot(-\rho\phi\langle\overline{\mathbf{u}'\mathbf{u}'}\rangle^{i}) - \\ -\rho\beta_\phi g\phi(\langle\overline{T_f}\rangle^{i} - T_{REF}) - \left[\frac{\mu\phi}{K}\overline{\mathbf{u}}_D + \frac{c_F\phi\rho|\overline{\mathbf{u}}_D|\,\overline{\mathbf{u}}_D}{\sqrt{K}}\right] \tag{12}$$

where the term $-\rho\beta_\phi g\phi(\langle\overline{T_f}\rangle^{i} - T_{REF})$ represents natural convection and uses the intrinsic averaged temperature of the fluid. The last two terms of equation (12) represent the total drag forces modelled by the Darcy and Forchheimer term. Symbol K represents medium permeability and c_F is the Forchheimer coefficient.

The term $-\rho\phi\langle\overline{\mathbf{u}'\mathbf{u}'}\rangle^{i}$ is the macroscopic Reynolds stress and can be obtained by:

$$-\rho\phi\langle\overline{\mathbf{u}'\mathbf{u}'}\rangle^{i} = \mu_{t_\phi}\,2\langle\overline{\mathbf{D}}\rangle^{v} - \frac{2}{3}\phi\rho\langle k\rangle^{i}\mathbf{I} \tag{13}$$

where

$$\langle\overline{\mathbf{D}}\rangle^{v} = \frac{1}{2}\left[\nabla(\phi\langle\overline{\mathbf{u}}\rangle^{i}) + [\nabla(\phi\langle\overline{\mathbf{u}}\rangle^{i})]^{T}\right] \tag{14}$$

represents the macroscopic deformation tensor, **I** is the unit tensor and μ_{t_ϕ} is the turbulent viscosity, which is modelled as:

$$\mu_{t_\phi} = \rho c_\mu \frac{\langle k\rangle^{i\,2}}{\langle\varepsilon\rangle^{i}} \tag{15}$$

where c_μ is a non-dimensional empirical constant. Hence, $\langle k\rangle^i$ and $\langle \varepsilon\rangle^i$ must be obtained through the transport equations in order to get μ_{t_ϕ}.

The macroscopic turbulent kinetic energy equation is:

$$\rho\left[\frac{\partial}{\partial t}(\phi\langle k\rangle^i)+\nabla\cdot(\overline{\mathbf{u}}_D\langle k\rangle^i)\right]=\nabla\cdot\left[(\mu+\frac{\mu_{t_\phi}}{\sigma_k})\nabla(\phi\langle k\rangle^i)\right]- \\ -\rho\langle\overline{\mathbf{u}'\mathbf{u}'}\rangle^i\nabla\overline{\mathbf{u}}_D+C_k\rho\frac{\phi\,k_\phi|\overline{\mathbf{u}}_D|}{\sqrt{K}}+G_\beta^i-\rho\phi\langle\varepsilon\rangle^i \tag{16}$$

where $\rho\langle\overline{\mathbf{u}'\mathbf{u}'}\rangle^i$ is defined by equation (13) and σ_k is a non-dimensional empirical constant. The term $G_\beta^i=\phi\frac{\mu_{t_\phi}}{\sigma_t}\beta_\phi^k\mathbf{g}\cdot\nabla\langle\overline{T}\rangle^i$ represents the generation of $\langle k\rangle^i$ due to natural convection, where $\beta_\phi=\frac{\langle\rho\beta(T-T_{ref})\rangle^v}{\rho\phi(\langle T\rangle^i-T_{ref})}$ is the macroscopic thermal expansion coefficient and $\beta_\phi^k=\frac{\langle\beta\overline{\mathbf{u}'T'}\rangle^v}{\phi(\overline{\mathbf{u}'T_f'})}$ is the macroscopic thermal coefficient.

The macroscopic turbulent kinetic energy dissipation equation is:

$$\rho\left[\frac{\partial}{\partial t}(\phi\langle\varepsilon\rangle^i)+\nabla\cdot(\overline{\mathbf{u}}_D\langle\varepsilon\rangle^i)\right]=\nabla\cdot\left[(\mu+\frac{\mu_{t_\phi}}{\sigma_\varepsilon})\nabla(\phi\langle\varepsilon\rangle^i)\right]+ \\ +c_1(-\rho\langle\overline{\mathbf{u}'\mathbf{u}'}\rangle^i\nabla\overline{\mathbf{u}}_D)\frac{\langle\varepsilon\rangle^i}{\langle k\rangle^i}+c_2C_k\rho\frac{\phi\,\varepsilon_\phi|\overline{\mathbf{u}}_D|}{\sqrt{K}}+c_1c_3G_\beta^i\frac{\langle\varepsilon\rangle^i}{\langle k\rangle^i}-c_2\rho\phi\frac{\langle\varepsilon\rangle^{i^2}}{\langle k\rangle^i} \tag{17}$$

where σ_ε, c_1, c_2 and c_3 are non-dimensional empirical constants.

2.4 Macroscopic energy equations

Using the time and volume average operators, described beforehand in equations (5) and (6), the macroscopic energy equations for the solid and fluid phase are obtained. After performing a volume integration over a REV the resulting equations are:
For the fluid phase

$$(\rho c_p)_f\left[\frac{\partial\phi\langle\overline{T}_f\rangle^i}{\partial t}+\nabla\cdot\left\{\phi\left(\langle\overline{\mathbf{u}}\rangle^i\langle\overline{T}_f\rangle^i+\langle{}^i\overline{\mathbf{u}}^i\overline{T}_f\rangle^i+\overline{\langle\mathbf{u}'\rangle^i\langle T_f'\rangle^i}+\langle\overline{{}^i\mathbf{u}'^iT_f'}\rangle^i\right)\right\}\right]= \\ =\nabla\cdot\left[k_f\nabla\left(\phi\langle\overline{T}_f\rangle^i\right)+\frac{1}{\Delta V}\int_{A_i}\mathbf{n}_i\,k_f\,\overline{T}_f\,dA\right]+\frac{1}{\Delta V}\int_{A_i}\mathbf{n}_i\,k_f\,\overline{T}_f\,dA \tag{18}$$

And for the solid phase:

$$(\rho c_p)_s\left\{\frac{\partial(1-\phi)\langle\overline{T}_s\rangle^i}{\partial t}\right\}=\nabla\cdot\left\{k_s\nabla\left[(1-\phi)\langle\overline{T}_s\rangle^i\right]-\frac{1}{\Delta V}\int_{A_i}\mathbf{n}_i\,k_s\overline{T}_s\,dA\right\}-\frac{1}{\Delta V}\int_{A_i}\mathbf{n}_i\,k_s\overline{T}_s\,dA \tag{19}$$

where A_i is the interfacial area inside the REV and $\mathbf{n}_i$ is the unit vector normal to the fluid-solid interface, pointing from the fluid to the solid phase. The intrinsic average temperatures of the solid and fluid phase, $\left\langle \overline{T}_s \right\rangle^i$ and $\left\langle \overline{T}_f \right\rangle^i$, need to be modelled to utilize equations (18) and (19).

For equation (18), the term $\left\langle {}^i\overline{\mathbf{u}}^i\overline{T}_f \right\rangle^i$ represents the thermal dispersion, $\overline{\langle \mathbf{u}' \rangle^i \langle T_f' \rangle^i}$ represents turbulent heat flow and $\left\langle \overline{{}^i\mathbf{u}'^i T_f'} \right\rangle^i$ turbulent thermal dispersion. These terms can be modelled using the following equations:

Thermal dispersion:

$$-\left(\rho c_p\right)_f \left(\phi \, \langle {}^i\overline{\mathbf{u}}^i \overline{T_f} \rangle^i \right) = \mathbf{K}_{disp} \cdot \nabla \langle \overline{T}_f \rangle^i \tag{20}$$

Turbulent heat flow

$$-\left(\rho c_p\right)_f \left(\phi \, \overline{\langle \mathbf{u}' \rangle^i \langle T_f' \rangle^i} \right) = \mathbf{K}_t \cdot \nabla \langle \overline{T}_f \rangle^i \tag{21}$$

Turbulent thermal dispersion:

$$-\left(\rho c_p\right)_f \left(\phi \, \langle \overline{{}^i\mathbf{u}' \, {}^i T_f'} \rangle^i \right) = \mathbf{K}_{disp,t} \cdot \nabla \langle \overline{T}_f \rangle^i \tag{22}$$

where $\mathbf{K}_{disp}$, $\mathbf{K}_t$ and $\mathbf{K}_{dispt}$ are, respectively, the thermal dispersion tensor, turbulent heat flow tensor and turbulent thermal dispersion tensor.

For both (18) and (19) equations the two terms on the right-hand side represent conduction and interfacial heat transfer, respectively. The conduction terms can be expressed by the following relationship:

$$\nabla . \left[\frac{1}{\Delta V} \int_{A_i} \mathbf{n}_i \, k_f \, \overline{T_f} \, dA \right] = \mathbf{K}_{f,s} \cdot \nabla \langle \overline{T}_s \rangle^i - \nabla . \left[\frac{1}{\Delta V} \int_{A_i} \mathbf{n}_i \, k_s \, \overline{T_s} \, dA \right] = \mathbf{K}_{s,f} \cdot \nabla \langle \overline{T}_f \rangle^i \tag{23}$$

where $\mathbf{K}_{f,s}$ and $\mathbf{K}_{s,f}$ are the local conduction tensors between fluid and solid.

The tensors $\mathbf{K}_{disp}$, $\mathbf{K}_t$, $\mathbf{K}_{dispt}$, $\mathbf{K}_{f,s}$ and $\mathbf{K}_{s,f}$ are denominated thermal conductivity tensors and can be associated by means of an effective thermal conductivity tensor for both the fluid ($\mathbf{K}_{eff,f}$) and the solid phase ($\mathbf{K}_{eff,s}$), as:

$$\mathbf{K}_{eff,f} = [\phi k_f] \, \mathbf{I} + \mathbf{K}_{f,s} + \mathbf{K}_{disp} + \mathbf{K}_{disp,t} + \mathbf{K}_t \tag{24}$$

$$\mathbf{K}_{eff,s} = [(1-\phi) k_s] \, \mathbf{I} + \mathbf{K}_{s,f} \tag{25}$$

where **I** is the unity tensor.

Interfacial heat transfer is represented by the last term on the right-hand side of equations (18) and (19) and can be modelled through a film coefficient h_i so that:

$$h_i a_i \left(\langle \overline{T_s} \rangle^i - \langle \overline{T_f} \rangle^i \right) = \frac{1}{\Delta V} \int_{A_i} \mathbf{n}_i \cdot k_f \nabla \overline{T_f} \, dA = \frac{1}{\Delta V} \int_{A_i} \mathbf{n}_i \cdot k_s \nabla \overline{T_s} \, dA \tag{26}$$

where $a_i = A_i / \Delta V$ is the superficial area per unit volume.

Finally, merging the terms in the macroscopic energy equations (fluid phase (18) and solid phase (19)) with equations (20), (21), (22), (23), (24), (25) and (26), an energy balance for each phase is obtained as:

$$\left\{(\rho c_p)_f \phi\right\}\frac{\partial\left\langle \overline{T}_f \right\rangle^i}{\partial t} + (\rho c_p)_f \nabla.\left(\mathbf{u}_D \left\langle \overline{T}_f \right\rangle^i\right) = \nabla.\left\{\mathbf{K}_{eff,f} \nabla\left\langle \overline{T}_f \right\rangle^i\right\} + h_i a_i \left(\langle \overline{T}_s \rangle^i - \langle \overline{T}_f \rangle^i\right) \quad (27)$$

$$\left\{(1-\phi)(\rho c_p)_s\right\}\frac{\partial\left\langle \overline{T}_s \right\rangle^i}{\partial t} = \nabla.\left\{\mathbf{K}_{eff,s} \nabla\left\langle \overline{T}_s \right\rangle^i\right\} - h_i a_i \left(\langle \overline{T}_s \rangle^i - \langle \overline{T}_f \rangle^i\right) \quad (28)$$

2.5 Numerical Method

Finite volume method (Patankar, 1980) with a collocated grid will be used for the discretization of the equations. SIMPLE algorithm will be used to correct the pressure field (to avoid issues with pressure field oscillations the velocities are obtained by individual interpolation, using discretized momentum equations on the nodes and the pressure differences across the faces are evaluated as in staggered grids). A hybrid interpolation scheme (Upwind(UDS) and central differences(CDS)) will be used for the convective terms. The implicit method will be used to evaluate the transient behavior of the system, with the equations being solved for both the present state t and the following state $t + \Delta t$. Results will be obtained by a numerical tool developed at LCFT/ITA.

2.6 Problem Description

Details of the thermocline are illustrated in Fig. 1. The tank has a d_t diameter, inlet and outlet with a d_e diameter and is filled with a porous ceramic material of height h_p. The entrance region is a clear medium of height h_l, hot air flows in through the inlet and heats the ceramic material up. The tank is axisymmetric. Simulation involving different porosities and boundary conditions will be analyzed.

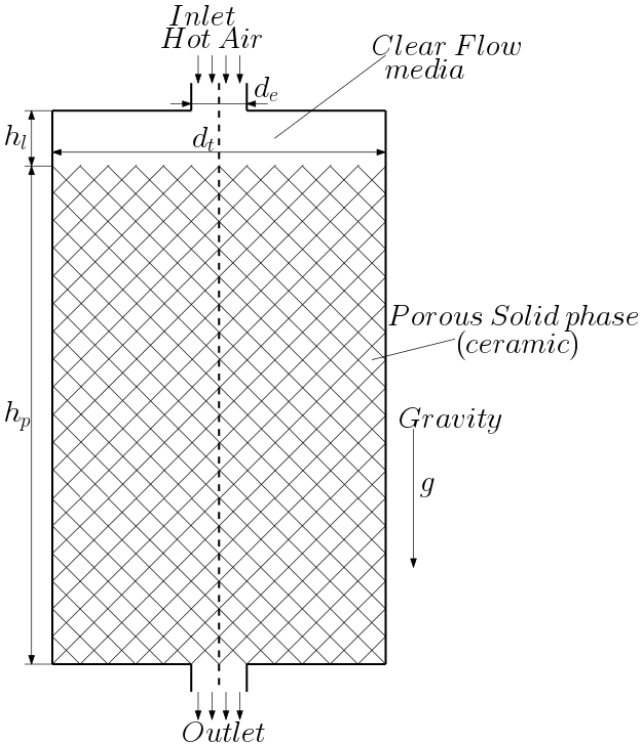

Figure 1. Thermocline scheme

3. PRELIMINARY RESULTS

The following figures demonstrate preliminary results for the charge cycle of the thermocline. The authors expect to analyze the data on the next iteration of the work.

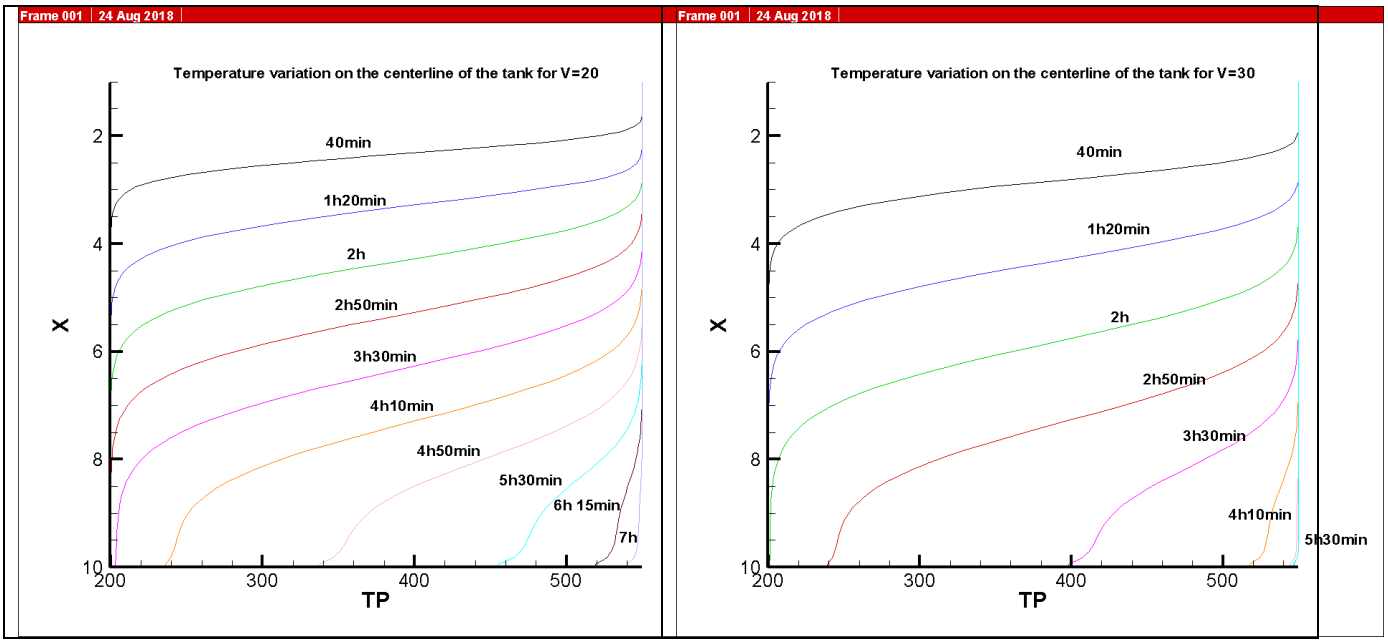

Figure 2. Temperature variantion on the centerline of the tank during the charging cycle for a) V=20 and b)V=30.

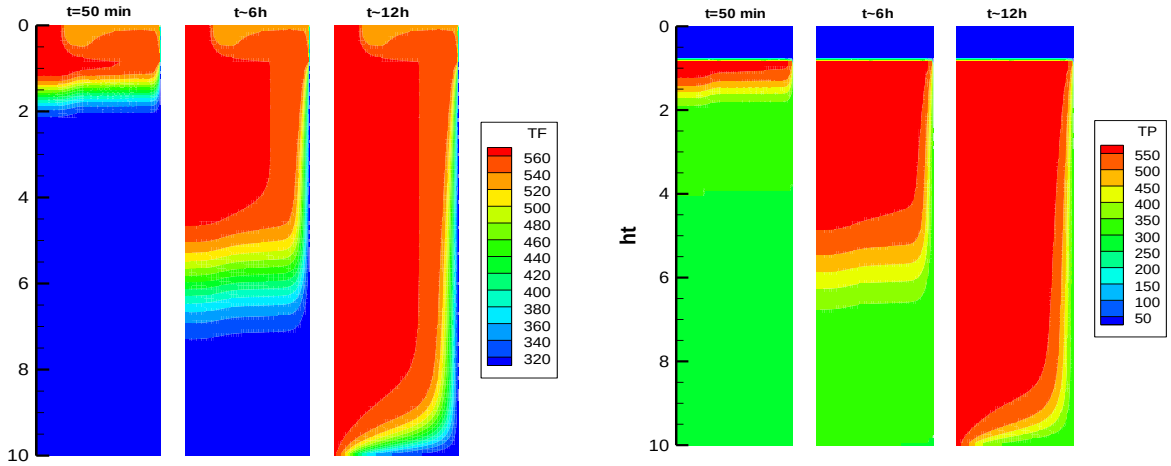

a) **b)**

Figura 3. Temperature variation through time for a case where h_t/d_t=2 with external convection on the tank walls a) for the fluid b) for the solid phase.

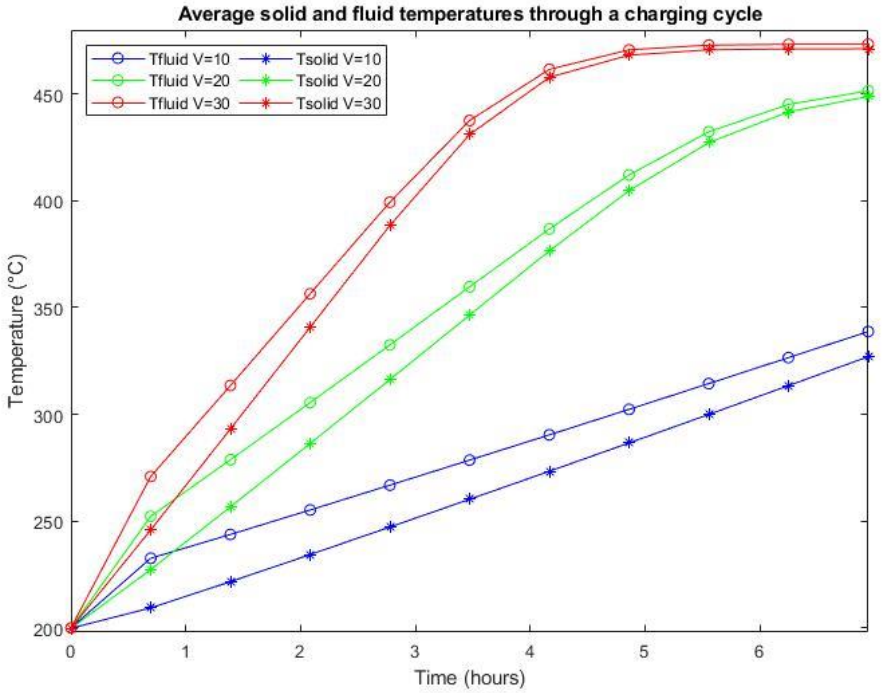

Figure 4. Average temperatures on the solid and fluid phases during the charging cycle for different inlet velocities.

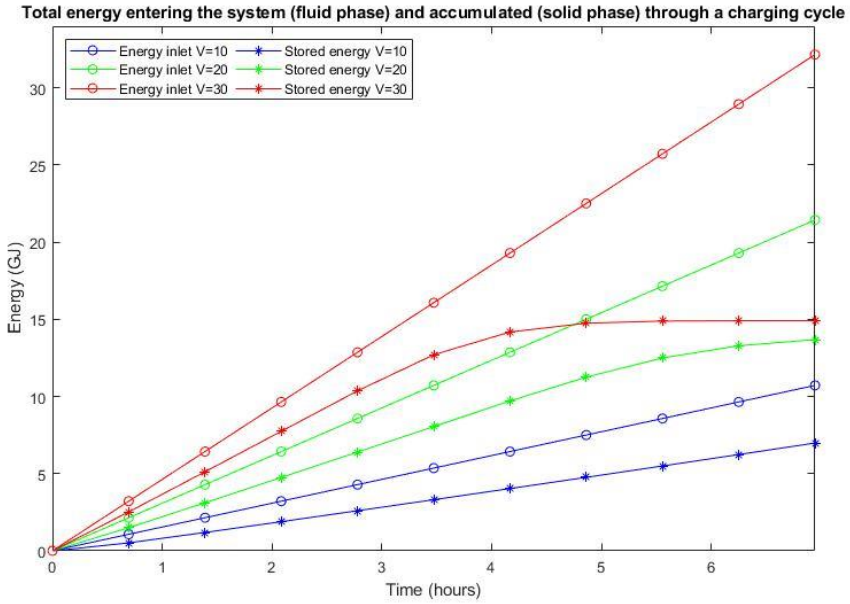

Figure 5. Total energy that enters the tank with the heated fluid phase and total energy accumulated by the porous matrix during the charging cycle for different inlet velocities.

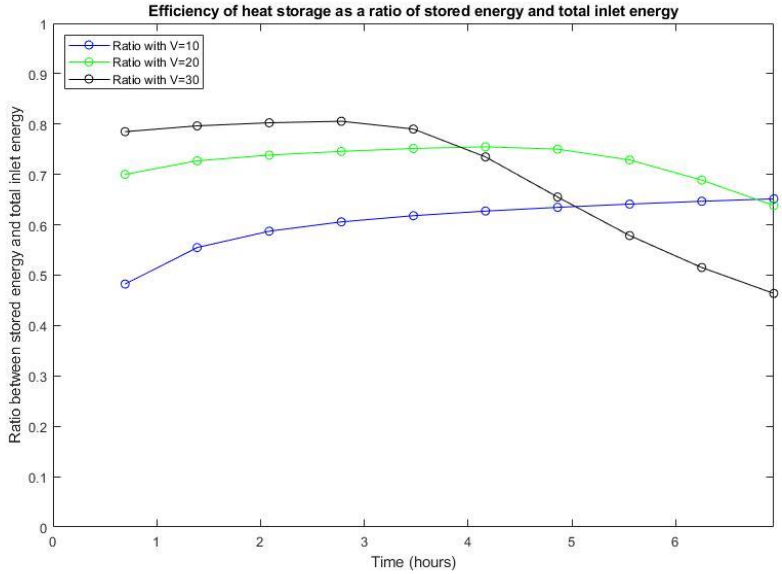

Figure 6. Ratio between the energy that was accumulated in the porous matrix and energy that enters the system with the fluid phase.

4. ACKNOWLEDGEMENTS

The authors are thankful to CAPES, Brazil, for their invaluable financial support during this research.

5. REFERENCES

Braga, E. J., & De Lemos, M. J. S. (2004). Turbulent natural convection in a porous square cavity computed with a macroscopic κ-ε model. *International Journal of Heat and Mass Transfer*, *47*(26), 5639–5650. https://doi.org/10.1016/j.ijheatmasstransfer.2004.07.017

EPE. (2015). *Projeção da demanda de energia elétrica para os próximos 10 anos (2015-2024). Nota Técnica DEA 22/12*. Rio de Janeiro. Retrieved from http://www.epe.gov.br/mercado/Documents/Série Estudos de Energia/20130117_1.pdf

Gray, W. G., & Lee, P. C. Y. (1977). On the theorems for local volume averaging of multiphase systems. *International Journal of Multiphase Flow*, *3*(4), 333–340. https://doi.org/10.1016/0301-9322(77)90013-1

International Energy Agency. (2016). Solar (PV and CSP). Retrieved December 14, 2016, from http://www.iea.org/topics/renewables/subtopics/solar/

Patankar, S. (1980). Numerical heat transfer and fluid flow. *Series in Coputational Methods in Mechanics and Thermal Sciences*. https://doi.org/10.1016/j.watres.2009.11.010

Pedras, M. H. J., & de Lemos, M. J. S. (2000). On the definition of turbulent kinetic energy for flow in porous media. *International Communications in Heat and Mass Transfer*.

Pedras, M. H. J., & de Lemos, M. J. S. (2001a). Macroscopic turbulence modeling for incompressible flow through undeformable porous media. *International Journal of Heat and Mass Transfer*, *44*(6), 1081–1093. https://doi.org/10.1016/S0017-9310(00)00202-7

Pedras, M. H. J., & de Lemos, M. J. S. (2001b). Simulation of Turbulent Flow in Porous Media Using a Spatially Periodic Array and a Low Re Two-Equation Closure. *Numerical Heat Transfer*, *39*(1), 35–59.

Pedras, M. H. J., & de Lemos, M. J. S. (2003). Computation of turbulent flow in porous media a low-Reynolds k-e model and an infinite array of transversally displaced elliptic rods. *Numerical Heat Transfer, Part A.*, *43*(6), 585–602. https://doi.org/10.1080/10407780390122970

de Lemos, M. J. S. (2012). Turbulence in Porous Media: Modeling and Applications (Second Edi). Elsevier Ltd. ISBN:9780080982410

Pilkington Solar International GmbH. (2000). Survey of Thermal Storage for Parabolic Trough Power Plants Period of

Performance : Survey of Thermal Storage for Parabolic Trough Power Plants Period of Performance. *NREL*, (September), 61. Retrieved from http://www.nrel.gov/csp/troughnet/pdfs/27925.pdf

Py, X., Azoumah, Y., & Olives, R. (2013). Concentrated solar power: Current technologies, major innovative issues and applicability to West African countries. *Renewable and Sustainable Energy Reviews*, *18*, 306–315. https://doi.org/10.1016/j.rser.2012.10.030

Rocamora, F. D., & de Lemos, M. J. S. (2000). Analysis of convective heat transfer for turbulent flow in saturated porous media. *International Communications in Heat and Mass Transfer*, *27*(6), 825–834. https://doi.org/10.1016/S0735-1933(00)00163-9

Saito, M. B., & de Lemos, M. J. S. (2010). A macroscopic two-energy equation model for turbulent flow and heat transfer in highly porous media. *International Journal of Heat and Mass Transfer*, *53*(11–12), 2424–2433. https://doi.org/10.1016/j.ijheatmasstransfer.2010.01.041

Santos, N. B., & de Lemos, M. J. S. (2006). Flow and Heat Transfer in a Parallel-Plate Channel with Porous and Solid Baffles. *Numerical Heat Transfer, Part A: Applications*, *49*(5), 471–494. https://doi.org/10.1080/10407780500325001

Xu, B., Li, P., & Chan, C. (2015). Application of phase change materials for thermal energy storage in concentrated solar thermal power plants : A review to recent developments, *160*, 286–307. https://doi.org/10.1016/j.apenergy.2015.09.016

6. RESPONSIBILITY NOTICE

The authors are the only ones responsible for the printed material included in this paper.